Kinematic synthesis, optimization and analysis of a non-anthropomorphic 2-DOFs wearable orthosis for gait assistance

Fabrizio Sergi, Dino Accoto, Nevio Luigi Tagliamonte, Giorgio Carpino,
Simone Galzerano and Eugenio Guglielmelli

Abstract— **This paper presents the kinematic optimization of a planar wearable active orthosis for hip and knee assistance during overground walking. A non-anthropomorphic design is pursued in order to improve ergonomics and to reduce torque requirements. A systematic search of the design space is performed and a selected generalized solution is optimized using genetic algorithms and constrained non-linear optimization. The design optimization method followed allows to conveniently re-distribute mechanical power through different actuators. Peak torque and velocity requirements for each actuator can be modulated, thus promoting a lighter design. A detailed analysis of the resulting mechanism workspace is carried out, including the evaluation of kinematic singularities, in order to verify the adequateness of the design in real-world scenarios. The developed model and results are validated through a numerical analysis and through experiments using a mock-up system.**

I. INTRODUCTION

Wearable Robots (WRs) are active mechanical systems worn by human operators to complement/substitute natural limbs functions (*orthotic robots*) or to replace missing limbs (*prosthetic robots*) [1]. *Exoskeletons* represent an instantiation of WRs. Their kinematic structure replicates the human anatomical one, since there exists a direct correspondence between robotic and human joints. Major challenges in terms of kinematic compatibility arise in the design of exoskeletons since a perfect match of the two kinematic structures in parallel cannot be fully achieved, due to the presence of *macro-misalignments* and *micro-misalignments* [2]. Such misalignments can cause the exchange of unwanted interaction forces causing discomfort or even pain for the subject [3], [4]. Non-anthropomorphic structures are instead inherently robust against alignment errors; significant improvements in ergonomics and kinematic compatibility are then expected from the use of such class of mechanisms. Moreover, the increased design freedom provided by this class of structures introduces the appealing opportunity of optimizing robot actuator requirements and dynamical properties. A proper placement of actuators can allow the exploitation of intrinsic dynamics in cyclic tasks as in [5] and the re-distribution among different actuators of torques required to support multiple human joints.

However, conventional design methods can be difficultly extended to the problem of designing non-anthropomorphic robots. This is due to the large number of open design parameters and to modeling issues related to the possible absence of closed-form solutions that solve in a general way the static forward and inverse kinematics problem of the resulting parallel structure composed of both human segments and robot links [6].

All the authors are with the Laboratory of Biomedical Robotics and Biomicrosystems, Center for Integrated Research (CIR), Università Campus Bio-Medico di Roma, Via Álvaro del Portillo, 21 - 00128 Roma, Italy.

Corresponding author: fabrizio.sergi@unicampus.it

This paper addresses the specific problem of the design of a WR for hip and knee assistance during gait in the sagittal plane. The pursued design is based on a systematic search of all admissible (i.e. kinematically compatible) solutions based on our previous work [7], and a kinematics-based design optimization is carried out to minimize static torques demanded to actuators during gait assistance.

II. METHODS

A. Problem definition

Based on the considerations above, the following hypotheses/constraints are imposed:

1) robot kinematic design is not fixed a-priori and can be possibly non-anthropomorphic;
2) the desired number of DOFs of the parallel structure comprising both human segments and robot links is two (*isostaticity* condition);
3) simultaneous and independent movements of the hip and the knee joints must not be constrained (i.e. the structure must not to impose unnatural kinematic constraints to the addressed human joints);
4) interaction with the human segments is based on pure forces applied to fixations along specified directions (Fig. 1);
5) in order to reduce the number of parameters of the design problem, only solutions involving revolute joints are considered.

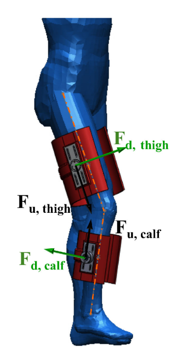

Fig. 1. Interaction forces between human segments and wearable robots. Desired forces ($\mathbf{F}_d$) are orthogonal to the addressed limbs axes, while undesired forces are shear forces on the human segments.

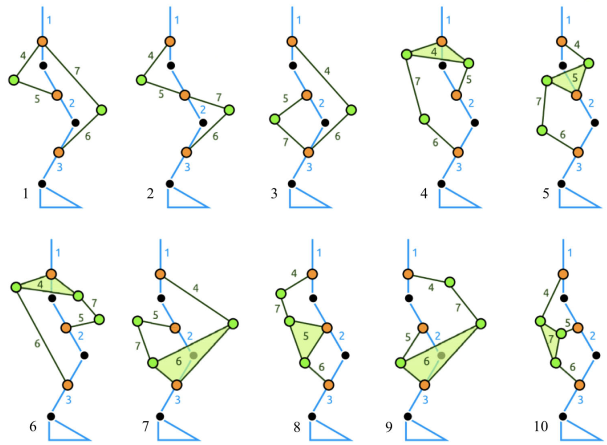

Fig. 2. Arbitrary morphological representations of the 10 generalized solutions for the design problem addressed. Human segments are reported in blue, and human articulations are reported in black. Robot joints are reported in orange (on attachment sites) and in green (adapted from [8]).

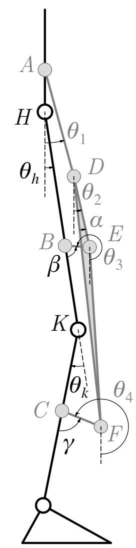

Length	Symbol
AH	l_1
DE	l_2
BE	l_3
HB	l_4
DF	l_5
FC	l_6
KC	l_7
AD	l_8
HK	h_1

Fig. 3. Kinematic scheme of the mechanism, including both human segments (black lines) and robot links (gray lines). Symbols for lengths and angles are reported. α is the angle $E\widehat{D}F$.

B. Kinematic synthesis

A graph-based method for the exhaustive enumeration of the generalized kinematic chains of planar non-anthropomorphic wearable robotic orthoses has been employed. The method includes two special tests: the HR-isomorphism test and the HR-degeneracy test, purposively devised to solve the problem of enumerating the set of admissible kinematic structures connected to a given set of human links and joints [7]. The method allowed to exhaustively list all the independent kinematic structures of planar kinematically-compatible wearable hip-knee robotic orthoses. Ten generalized solutions (topologies) are admissible in the considered design case, as shown in Fig. 2. Such solutions represent the most synthetic form of describing the mechanical optimization problem described so far.

In the present work, we applied a preliminary optimization criterion based on a basic static ergonomics principle: correct force interaction in WRs is based on the transfer of forces to human segments only in the direction orthogonal to the bones ($\mathbf{F}_d$ forces reported in Fig. 1. If the connection between a human segment and the robot is implemented through a binary passive link (i.e. with two unactuated revolute joints at its extremities), static forces applied on the human segments are necessarily directed along the connection link axis. No forces along the orthogonal direction can be present, since no torque can be applied by passive joints. If said passive link is orthogonal to the human segment to which it is connected, the transfer of forces can be statically optimized based on simple geometric considerations (i.e. the attached link is orthogonal to the addressed segment).

Using this criterion, we investigated which of the 10 topologies in Fig. 2 allowed links 5 and 6 (connected to the thigh and shank respectively) to be completely passive and orthogonal to human segments (labeled with 2 and 3). Three topologies (4, 6 and 10) guarantee in principle such condition, while still allowing independent control of hip and knee movements by actuating the two remaining joints. Topology 10 was finally selected, since it allows to reduce size and weight and to better distribute masses and inertias along the lower limb. A schematic of the resulting kinematic chain is shown in Fig. 2.

C. Kinematic model

A kinematic model has been derived, based on the schematic shown in Fig. 3. The following four scalar closure equations can be formulated:

$$\begin{aligned} l_8 \mathrm{c}\theta_1 + l_2 \mathrm{c}\theta_2 + l_3 \mathrm{c}\theta_3 - l_1 - l_5 \mathrm{c}\theta_h &= 0 \\ l_8 \mathrm{s}\theta_1 + l_2 \mathrm{s}\theta_2 + l_3 \mathrm{s}\theta_3 - l_5 \mathrm{s}\theta_h &= 0 \\ l_8 \mathrm{c}\theta_1 + l_5 \mathrm{c}(\theta_2 - \alpha) + l_6 \mathrm{c}\theta_4 - l_1 - h_1 \mathrm{c}\theta_h - l_7 \mathrm{c}\theta_{hk} &= 0 \\ l_8 \mathrm{s}\theta_1 + l_5 \mathrm{s}(\theta_2 - \alpha) + l_6 \mathrm{s}\theta_4 - h_1 \mathrm{s}\theta_h - l_7 \mathrm{s}\theta_{hk} &= 0 \end{aligned} \tag{1}$$

where the short-hand notation $\mathrm{c}\theta_i$ is intended for $\cos\theta_i$ and θ_{hk} is intended for $\theta_h - \theta_k$.

The system (1) includes 9 geometric parameters related to robot design ($l_{1,...,8}$ and α), 1 parameter describing human anatomy (h_1) and 6 unknonwn variables $\theta_{1,...,4}$, θ_h and θ_k. In the model, actuators are in joints A and D (corresponding actuated links angles relative to the fixed frame θ_1 and θ_2. The desired effect is to provide support to human joints H (hip) and K (knee), with rotations θ_h and θ_k. The inverse kinematics problem consists in obtaining the mathematical expression for the set of 2D functions (surfaces) f_1 and f_2, that allows to calculate which angle of the actuated joints θ_1 and θ_2 are required to achieve the resulting rotations on the human joints θ_h and θ_k, so that:

$$\theta_1 = f_1(\theta_h, \theta_k) \tag{2}$$

$$\theta_2 = f_2(\theta_h, \theta_k) \tag{3}$$

Conversely, the forward kinematics problem consists in obtaining the mathematical expression for the surfaces g_1 and g_2, that allows to compute the human joints rotations based on the actuated joints measurements, so that:

$$\theta_h = g_1(\theta_1, \theta_2) \tag{4}$$
$$\theta_k = g_2(\theta_1, \theta_2) \tag{5}$$

It was not possible to obtain a sufficiently manageable closed-form solution for equations (2) to (5). However, this mechanism is still very appealing for the wearable robotics application described. For this reason, it was then decided to solve the kinematic problems using an approximation method. The system of equations (1) was solved numerically and an approximated form of functions f_i and g_i, $i = 1, 2$ was obtained using 2D polynomial fitting. The system of equations was solved using the MATLAB™ function `fsolve`, starting from the initial configuration C_0 shown in Table I, and angles calculated in a generic posture of the gait cycle [9].

A rectangular grid of hip and knee angles was constructed, taking into account the normal walking kinematic profiles reported in [9] and extending the domain of existence of the human joints angles in order to take into account for inter-subjects variability in the nominal walking pattern. A grid of admissible hip and knee postures was then defined by the 50-elements linearly spaced vectors $\theta_{h,grid}$ and $\theta_{k,grid}$, and for each combination of hip and knee angles the solutions of the inverse kinematics problem was calculated numerically. Analogously, a grid was constructed based on the angles θ_1 and θ_2 obtained through inverse kinematics and the system was solved to obtain the values of θ_h and θ_k for every combination of actuated joints positions. The obtained data-set were fitted through 3rd order, 2-variables polynomials using least-squares minimization, in the form of:

$$\begin{aligned}\hat{\theta}_1 = a_{1,0} + a_{1,1}\theta_h + a_{1,2}\theta_k + a_{1,3}\theta_h^2 + a_{1,4}\theta_h\theta_k + ...\\ ... + a_{1,5}\theta_k^2 + a_{1,6}\theta_h^3 + a_{1,7}\theta_h^2\theta_k + a_{1,8}\theta_h\theta_k^2 + a_{1,9}\theta_k^3\end{aligned} \tag{6}$$

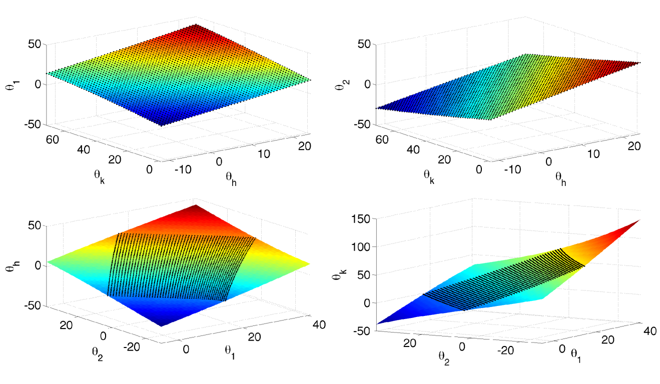

Fig. 4. Solutions of the forward and inverse kinematics problem for the initial model (configuration C_0 in Table I). Solutions of equations (1) are represented with black dots, while values obtained through 3rd order polynomial fitting (10 parameters for each data set) are represented through colormap surfaces. Minimum adjusted R-square value: 0.999 for $\hat{\theta}_h$, maximum RMS error: 0.06 deg, for $\hat{\theta}_k$.

This allowed to obtain a highly accurate approximation of functions f_1, f_2, g_1 and g_2 (maximum residual: 0.15 deg, RMS error: 0.06 deg) amenable to analytical operations, such as differentiation (see Fig. 4), that was employed to obtain the relations of forward differential kinematics, i.e.:

$$\begin{bmatrix} \dot{\theta}_h \\ \dot{\theta}_k \end{bmatrix} = \hat{\mathbf{J}}(\theta_1, \theta_2) \begin{bmatrix} \dot{\theta}_1 \\ \dot{\theta}_2 \end{bmatrix}, \tag{7}$$

where the analytic Jacobian $\hat{\mathbf{J}}$ was computed by differentiating the approximated expression of functions g_1 and g_2, obtained through polynomial fitting.

The knowledge of an analytical, configuration-dependent form of the Jacobian matrix allows to calculate the torques required to actuated joints τ_1 and τ_2 to verify the static equilibrium, in presence of torques applied to hip and knee joints, τ_h and τ_k, so that:

$$\begin{bmatrix} \tau_1 \\ \tau_2 \end{bmatrix} = \hat{\mathbf{J}}^T(\theta_1, \theta_2) \begin{bmatrix} \tau_h \\ \tau_k \end{bmatrix}, \tag{8}$$

Considering the following kinematic relations for the rotation of actuated joints:

$$\begin{aligned}\theta_{m_1} &= \theta_1 \\ \theta_{m_2} &= \theta_2 - \theta_1\end{aligned} \tag{9}$$

it is possible to verify that the torques supplied by motors m_1 and m_2 on joints A and D, respectively, are:

$$\begin{aligned}\tau_{m_1} &= \tau_1 + \tau_2 \\ \tau_{m_2} &= \tau_2\end{aligned} \tag{10}$$

D. Design optimization

The model derived in (1)–(10) was used to optimize the design. The main goal of the optimization was to reduce the torque required to actuators to support normal locomotion. A scalar objective function was defined, based on known technological limitations of actuators. The objective function minimizes the peak torque required to actuators, and also high frequency content of torques required to provide support during the gait cycle. Equations (8) and (10) were applied, using the profiles calculated through inverse-dynamics in standard walking data-sets [9] as input torques $\tau_h(t)$ and $\tau_k(t)$. Said $p_{m_i}(f)$ the power spectral density corresponding to the signal $\tau_{m_i}(t)$, the power P_{m_i} for frequencies lower than f is:

$$P_{m_i}(f) = \int_0^f p_{m_i}(\phi) d\phi, \tag{11}$$

and the normalized power $\breve{P}_{m_i}(f)$, is defined as:

$$\breve{P}_{m_i}(f) = \frac{P_{m_i}(f)}{P_{m_i}(\infty)} \tag{12}$$

Since the main limitations of actuation systems for wearable robotics applications are provided by limited peak torque and torque regulation bandwidth, the following fitness functions were defined:

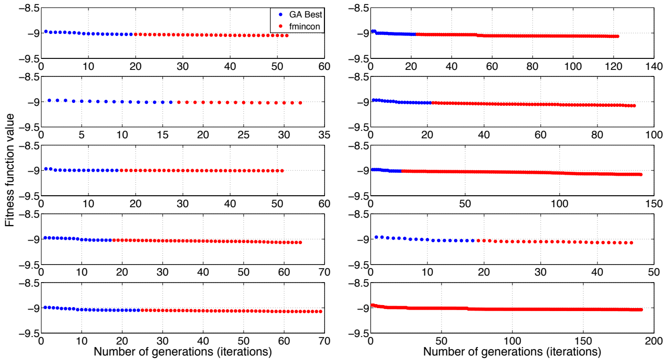

Fig. 5. Result of the optimization process, in terms of the fitness function defined in eq. (16).The top-most four rows correspond to eight different runs of the algorithm, using random initial conditions in the search domain. The bottom row reports the results of an optimization which starts from the the initial configuration C_0 (fitness value: -6.94); in the left C_0 is one of the individuals of the GA, in the right C_0 is the starting point of the CNLO.

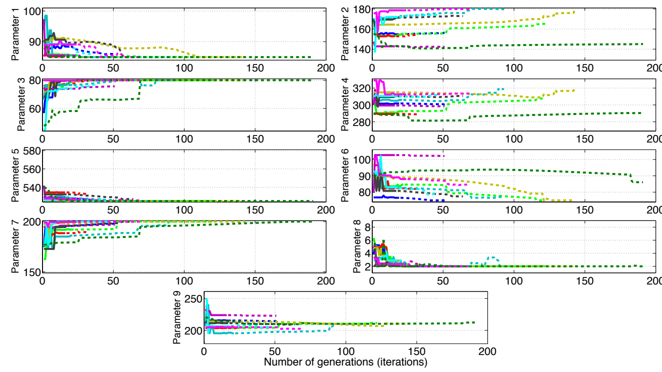

Fig. 7. Optimized design variables. Every plot describes the value of the specific design parameter. Different colors represent the different runs of the optimization. Continuous lines refer to the best individual produced by the GA at one generation, dotted lines correspond to the value of the solution calculated through CNLO at one iteration.

$$fitness_{peak} = \max(\tau_{m_1}(t), \tau_{m_2}(t))/\tau_{max} \quad (13)$$

$$fitness_{pow_1} = -\breve{P}_{m_1}(f_0)/\breve{P}_{max} \quad (14)$$

$$fitness_{pow_2} = -\breve{P}_{m_2}(f_0)/\breve{P}_{max} \quad (15)$$

having set $\tau_{max} = 50$ N·m, $f_0 = 5$ Hz and $\breve{P}_{max} = 0.95$. Equation (13) depends on the peak static torque required to one of the actuators during gait, while (14) and (15) describe the relevance of frequency content to torque support for frequencies below 5 Hz.

Functions (13) to (15) have finally been condensed in a single scalar fitness function, defined as:

$$fitness = fitness_{peak} + w \cdot (fitness_{pow_1} + fitness_{pow_2}) \quad (16)$$

For the aims of this paper, the parameter w has been set to 5. A hybrid optimization strategy has been employed in order to explore the 9-dimensional space defined by parameters ($l_1, ..., l_8, \alpha$), whose domain of existence is defined in Table I. The optimization algorithm consists of the consecutive application of a Genetic Algorithm (GA)[1] and a deterministic constrained non-linear optimization (CNLO) method (using MATLAB `fmincon` function[2]). The latter was used to performe a local optimization, using the best individual produced by the Genetic Algorithm as starting point. Results corresponding to ten different optimization runs are shown in Fig. 5; eight runs used random initial conditions, while two apply the optimization starting from the initial configuration C_0.

Variability of the 10 solutions obtained is small in terms of fitness function values (-9.05 ± 0.02, with peak torques 51.5 ± 0.3 N·m, $p < 0.05$), while values of optimized parameters can vary as much as 30% of their domain of existence, as shown in Fig. 7, indicating that not all of the design parameters have the same relevance in terms of design optimization. The fittest solution (C_{OPT}, parameters reported in Table I, fitness function value -9.08) was selected for the final design, and the torque profiles required to actuators during a walking cycle are shown in Fig. 6.

E. Kinematic analysis

The produced configuration was analyzed so to guarantee that no kinematic singularity can occur during the gait cycle. As it can be seen from the model shown in Fig. 3, the same hip and knee posture could in principle be obtained with the robot in 4 different configurations, depending on the values of relative angles β and γ. For each posture, links BE and FC could point either in the forward or backward direction

[1]GA parameters: Population Size: 40, Max Generations: 100, Scattered Crossover with Fraction 0.8, Elite count:2, Migration Fraction: 0.4, Migration Interval: 5, Stall Generations Limit: 15, Function Tolerance: 10^{-5}

[2]The "active-set" algorithm was used. Maximum number of iterations: 100, Parameters Termination Tolerance: 10^{-9}

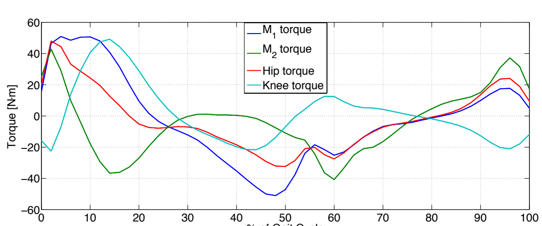

Fig. 6. Torque profiles required to actuators in the optimized configuration C_{OPT} and torque profiles calculated through inverse-dynamics in the gait data-set [9], for a subject's mass of 80 kg.

TABLE I

PARAMETERS VALUES AND BOUNDARIES

	l_1	l_2	l_3	l_4	l_5	l_6	l_7	α	l_8
min	85	130	45	270	525	75	150	2	180
max	100	180	80	330	580	120	200	8	260
C_0	90	155	48	290	540	90	177	5.5	220
C_{OPT}	85	180	80	320	525	75	200	2	210

relative to the shank and thigh segments, respectively. This implies that the system can be in one of the following kinematic configurations:

1) $0 < \beta < \pi$ and $0 < \gamma < \pi$
2) $\pi < \beta < 2\pi$ and $0 < \gamma < \pi$
3) $0 < \beta < \pi$ and $\pi < \gamma < 2\pi$
4) $\pi < \beta < 2\pi$ and $\pi < \gamma < 2\pi$

All conditions 1) to 4) were systematically explored, by solving the system of equations (1), using as starting points configurations satisfying one of the specific conditions at a time and verifying later if the obtained solution (if any) verified the specific condition on angles β and γ. For each of the four conditions, a set of solutions $\theta_{\mathbf{sol,i}} = [\theta_1\ \theta_2\ \theta_3\ \theta_4]$, i =1, 2, 3, 4 of equations (1) was calculated, giving as input all combinations of θ_h and θ_k in the rectangular 100×100 grid of equally spaced vectors $-25 \leq \theta_h \leq 25$, $-5 \leq \theta_k \leq 97$. Based on the obtained solutions, the condition of flipping between configurations i and j can be expressed through the binary variable $flip_{i,j}$, defined as:

$$flip_{i,j}(\theta_h, \theta_k) = \text{norm}[\theta_{\mathbf{sol,i}}(\theta_\mathbf{h}, \theta_\mathbf{k}) - \theta_{\mathbf{sol,j}}(\theta_\mathbf{h}, \theta_\mathbf{k})] < \epsilon, \tag{17}$$

where ϵ is a small-enough number that depends on solver approximations. If the same state is present at the boundaries of the domains of existence of a couple of different configurations, the mechanism can switch from one configuration to the other. This would imply the impossibility to completely control the evolution of the system by regulating only actuators torque/position. Since in normal conditions the mechanism is always in condition 1), it is exhaustive to verify the values of the variable $flip_{1,k}$, with k = 1, 2, 3 (i.e. the possibility of the mechanism to switch from configuration 1) to the others).

This analysis is reported in Fig. 8 for the optimized configuration C_{OPT}, that shows that no flipping can occur between configurations 1) and 2) in the range considered, there is not any admissible hip and knee posture that verifies (17). The same analysis was conducted for $flip_{1,3}$ and $flip_{1,4}$ showing the same result.

III. DESIGN VALIDATION

The described kinematic modeling method has been validated both through numerical simulations and through experimental tests, using a purposively developed, 2:1-scaled mockup system nicknamed Benino (fig. 10(a)). The system has been developed so to provide a real-world demonstration of the adequateness of the modelling approach, with specific reference to the lack of kinematic singularities during gait. Benino is based on configuration C_0 and actuated by 50 W gearmotors (Maxon Motors Inc.) which include 10 bits incremental encoders to measure angles θ_1 and θ_2. Two absolute 15 bit rotary encoders (Gurley Precision Instruments) are applied on human joints to measure hip and knee angles and are used to benchmark the position control scheme. A position control scheme has been used, based on the minimization of the error $\mathbf{e}(t)$, defined as:

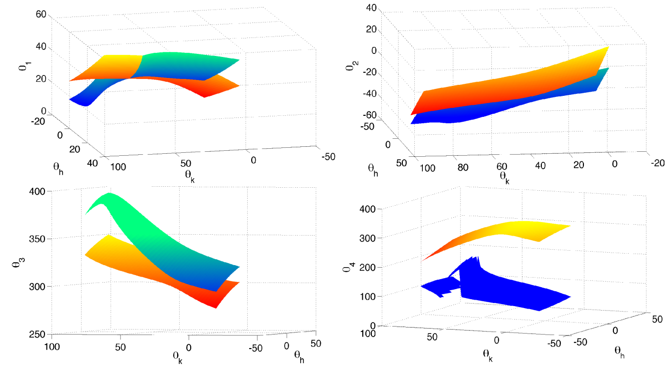

Fig. 8. Solution of the inverse kinematics problem in terms of angles $\theta_{1,\dots,4}$, for configuration 1) (red-yellow colormap) and configuration 2) (blue-green colormap). The two states are not contiguous (i.e. it is not possible to flip from one configuration to another) in the range of hip and knee postures considered: $-25 \leq \theta_h \leq 25$, $-5 \leq \theta_k \leq 97$, since the condition reported in eq. (17) is never verified.

$$\mathbf{e}(t) = \begin{bmatrix} \hat{\theta}_h(t) - \theta_{h,des}(t) \\ \hat{\theta}_k(t) - \theta_{k,des}(t) \end{bmatrix}, \tag{18}$$

where $\hat{\theta}_h(t)$ is the estimated hip angle obtained through polynomial fitting of equation (4) using measurements of the actuated angles θ_1 and θ_2, and $\theta_{h,des}(t)$ is the desired hip motion. The position control scheme is based on the transpose of the approximated Jacobian $\hat{\mathbf{J}}(\mathbf{q})$, $\mathbf{q} = (\theta_1,\, \theta_2)^T$ and is such that the commanded positions at the step t_{k+1} are given by:

$$\mathbf{q}(t_{k+1}) = \mathbf{q}(t_k) + \dot{\mathbf{q}}(t_k), \tag{19}$$

with

$$\dot{\mathbf{q}}(t_k) = \hat{\mathbf{J}}^\mathbf{T}(\mathbf{q}(t_k))\,\mathbf{K}\,\mathbf{e}(t_k). \tag{20}$$

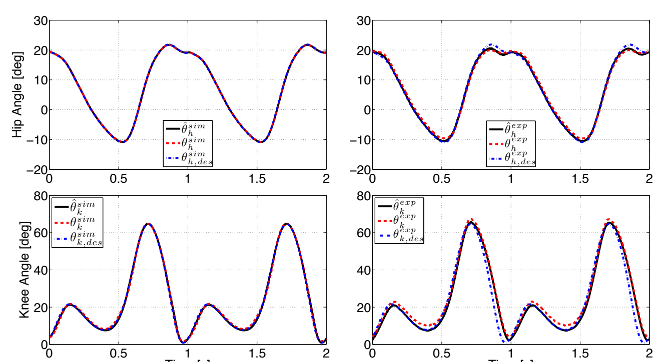

Fig. 9. Performances of the described position control scheme, based on the polynomial fitting estimation of $\mathbf{J}(\theta_1, \theta_2)$. The left plots report results obtained in simulations, while the right plots report the results obtained experimentally using the mockup. $\theta_{h,k}^{sim}$ are the angles obtained through numerical solution of the inverse kinematics problem. $\theta_{h,k}^{exp}$ are the angles measured through the absolute encoders mounted on human joints. $\hat{\theta}_{h,k}$ are the angles estimated through polynomial fitting and are used as control variables in (18)-(20) in both cases.

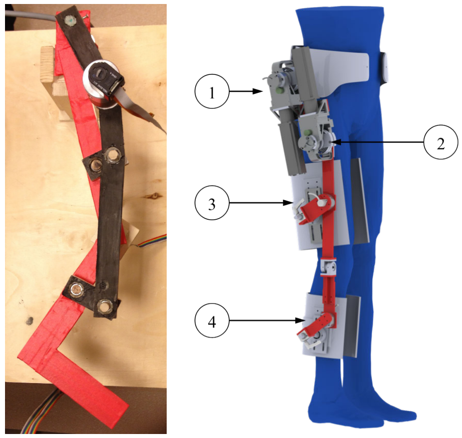

(a) (b)

Fig. 10. (a) Benino, the wooden 2:1 scale mockup of configuration C_0. Human segments are in red, robot links are in black. Gearmotors include incremental encoders to measure angles θ_1 and θ_2. Absolute angular encoders (not visible in the picture) are co-located with the mockup hip and knee joints. (b) 3D rendering representing a preliminary design based on the optimized configuration C_{OPT}. 1 and 2: Series Elastic Actuators; 3 and 4: thigh and shank cuffs.

The results of the position regulation scheme, as obtained through numerical analysis and experimentally using the mockup system, are reported in Fig. 9. The RMS error of position regulation is 0.12 deg for the hip joint and 0.4 deg for the knee joint in simulations. Position regulation performances were slightly lower in the mockup system developed. The hip RMS error obtained is of 0.6 deg, while a higher value (3.5 deg) was obtained for the knee joint. This is mainly due to the velocity limitations of the actuators employed, as it can be seen from the top-right plot in Fig. 9, that shows a noticeable difference in the maximum velocity of the desired and actual knee profiles. In both cases, the errors related to the kinematic model used ($\hat{\theta}_{h,k} - \theta_{h,k}$) were negligible (RMS value around 0.2 deg, with peak values of 0.6 deg).

IV. CONCLUSIONS AND FUTURE WORK

This paper addressed the specific problem of the design of a WR for hip and knee assistance during gait in the sagittal plane. A design based on a systematic search of all admissible solutions was pursued, and a design optimization employed so to minimize torques required to actuators for hip and knee gait assistance. A kinematic modeling method based on the polynomial fitting approximation of the forward and inverse kinematic problems has been presented and applied to the optimization problem. An extensive kinematic analysis has been performed, in order to rule out the existence of kinematic singularities throughout the workspace. The developed model and results have been validated through both a numerical analysis and experiments using a mockup.

Torque profiles required to actuators have higher peak torques, compared to an ideal anthropomorphic case, with massless robot parts. However, the design optimization method followed allows to conveniently re-distribute mechanical power through different actuators. Peak torque and velocity requirements for each actuator can be modulated, thus promoting a lighter design. Moreover, the pursued design avoids the presence of actuators in distal portions of the lower limb, thus reducing the inertial effects reflected on the subject during gait assistance, as it is the case of anthropomorphic robots for knee assistance. To the authors' knowledge, it is the first time that the described design approach has been used for the design of a wearable robot. This paper gives a first preliminary evidence of the advantages of a non-anthropomorphic design in terms of actuation requirements.

The optimization considered in this paper was limited to kinematics. Future work will also take into account dynamical factors that are crucial during legged locomotion [5]. To this aim, a dynamical model of the system will be developed and the optimization process will be adapted accordingly. The optimized solution is being engineered in a WR prototype, which includes custom-developed Series Elastic Actuators [10] and carbon-fiber connection cuffs (Fig. 10(b)). Future work will also include the development and testing of such bilateral non-anthropomorphic wearable orthosis for gait assistance.

V. ACKNOWLEDGMENT

This work was supported by the FP7 FET Proactive Initiative "Embodied Intelligence" of the European Commission, project no. ICT-2007.8.5-231451 - EVRYON (EVolving morphologies for human-Robot sYmbiotic interactiON).

REFERENCES

[1] J. L. Pons, *Wearable Robots: Biomechatronic Exoskeletons*. Wiley, 2008.

[2] A. Schiele and F. C. van der Helm, "Kinematic design to improve ergonomics in human machine interaction," *IEEE Trans Neural Syst Rehabil Eng*, vol. 14, no. 4, pp. 456–69, Dec 2006.

[3] G. Colombo, M. Jorg, and V. Dietz, "Driven gait orthosis to do locomotor training of paraplegic patients," *Engineering in Medicine and Biology Society, 2000. Proceedings of the 22nd Annual International Conference of the IEEE*, vol. 4, pp. 3159 – 3163 vol.4, 2000.

[4] N. Jarrassé, M. Tagliabue, J. V. G. Robertson, A. Maiza, V. Crocher, A. Roby-Brami, and G. Morel, "A methodology to quantify alterations in human upper limb movement during co-manipulation with an exoskeleton." *IEEE Trans Neural Syst Rehabil Eng*, vol. 18, no. 4, pp. 389–97, 2010.

[5] S. Collins, A. Ruina, R. Tedrake, and M. Wisse, "Efficient Bipedal Robots Based on Passive-Dynamic Walkers," *Science*, vol. 307, no. 5712, pp. 1082–1085, Feb. 2005.

[6] L. W. Tsai, *Robot analysis: the mechanics of serial and parallel manipulators*. Wiley-Interscience, 1999.

[7] F. Sergi, D. Accoto, N. Tagliamonte, G. Carpino, and E. Guglielmelli, "A systematic graph-based method for the kinematic synthesis of non-anthropomorphic wearable robots for the lower limbs," *Frontiers of Mechanical Engineering*, vol. 6, pp. 61–70, 2011.

[8] J. van den Kieboom, F. Sergi, D. Accoto, E. Guglielmelli, R. Ronsse, and A. J. Ijspeert, "Co-evolution of morphology and control of a wearable robot for human locomotion assistance exploiting variable impedance actuators," *Procedia Computer Science*, vol. 7, no. 0, pp. 223 – 225, 2011.

[9] D. Winter, *Biomechanics and Motor Control of Human Movement*. Wiley, 2009.

[10] F. Sergi, D. Accoto, G. Carpino, N. L. Tagliamonte, and E. Guglielmelli, "Design and characterization of a compact rotary series elastic actuator for knee assistance during overground walking," *submitted to the IEEE RAS/EMBS International Conference on Biomedical Robotics and Biomechatronics, 2012, Rome*, 2012.